FATIGUE ANALYSIS OF WECS COMPONENTS USING A RAINFLOW COUNTING ALGORITHM*

Herbert J. Sutherland
and
Larry L. Schluter
Wind Energy Research Division
Sandia National Laboratories
Albuquerque, NM 87185

SAND--90-1149C

DE91 000774

ABSTRACT

A "rainflow counting algorithm" has been incorporated into the LIFE2 fatigue/fracture analysis code for wind turbines. The count algorithm, with its associated pre- and post-count algorithms, permits the code to incorporate time-series data into its analysis scheme. After a description of the algorithms used here, their use is illustrated by the examination of stress-time histories from the Sandia 34-m Test Bed vertical axis wind turbine. The results of the rainflow analysis are compared and contrasted to previously reported predictions for the service lifetime of the fatigue critical component for this turbine.

INTRODUCTION

The analysis of the fatigue lifetime of a component for a Wind Energy Conversion System (WECS) requires that the stress state imposed upon that component be formulated in terms of stress cycles. Most data acquisition systems and some structural analysis techniques yield data that are a function of time. Thus, to use stress-time histories for fatigue analysis requires that the data be converted into stress cycles. One commonly used algorithm that performs this conversion is the "rainflow counting algorithm" that has been described by Downing and Socie [1].

This algorithm, with its associated pre- and post-count algorithms, has been incorporated into the LIFE2 fatigue/fracture analysis code for wind turbines [2,3]. Complete descriptions of the algorithms and the numerical techniques used to implement them are contained in References 4, 5 and 6. A "User's Manual" for this additional feature of the LIFE2 code is also provided in Reference 5.

After a discussion of the algorithms incorporated into the LIFE2 code, their use is illustrated by the examination of stress-time histories from the Sandia 34-m Test Bed Vertical Axis Wind Turbine (VAWT). The results of the rainflow analysis are then compared and contrasted to previously reported predictions for the service lifetime of this turbine [7].

RAINFLOW COUNTING ALGORITHM

The rainflow counting algorithm [1] defines a stress cycle to be a closed stress/strain hysteresis loop. The algorithm characterizes each stress cycle in a histogram by its mean value and its peak-to-peak range. Pre- and post-count algorithms are used to support and enhance the operation of the rainflow counter and to format its output for analysis by the code. Complete descriptions of the algorithms and the numerical techniques used to implement them are contained in References 4, 5 and 6.

The LIFE2 Code

The LIFE2 computer code is a fatigue/fracture analysis code specifically designed for the analysis of wind turbine components [2,3]. It is a PC-compatible, Fortran code that is written in a top-down modular format with a "user friendly," interactive interface. In this numerical formulation, an "S-n" fatigue analysis is used to describe the initiation, growth and coalescence of micro-cracks into macro-cracks. A linear, "da/dn" fracture analysis is used to describe the growth of a macro-crack.

Pre-Count Algorithms

Several auxiliary algorithms are used to support the rainflow counter. The initial set of algorithms prepares the data for the rainflow counter by identifying the peaks and valleys (extrema) contained in the data and discarding "small" stress cycles.

To illustrate the use of this set of algorithms, consider the typical stress-time history shown in Figure 1. The first algorithm identifies peaks and valleys in the data record by scanning for changes in the sign of the slope between successive data points. Typically, the data contained in this class of stress records are

*This work is supported by the U.S. Department of Energy at Sandia National Laboratories under contract DE-AC04-76DP00789.

taken at uniform time intervals. This constant-time-interval sampling technique, may or may not record actual extrema in the data, because the extrema may have been cropped or "squared off," e.g., see the peak that occurs near 82.4 seconds in Figure 2 (Figure 2 is an expanded view of Figure 1). To obtain a better estimate of the actual extreme value at a slope change, an optional interpolation algorithm may be invoked. The algorithm fits a parabola to the three data points nearest each change in slope to estimate the actual extrema. The estimated maximum for the peak near 82.4 seconds is shown as a triangle in Figure 2. As shown by the other peaks and valleys in Figure 2 and 3, if the extrema have not been squared off, the algorithm returns values very near the extrema recorded in the data record (also shown as triangles in the figures).

For the 80 to 100 second section of the data record shown in Figure 1, these algorithms selected the extrema shown as triangles in Figure 3. As seen in this figure, a large number of small cycles have been identified. These cycles may be eliminated from further consideration by employing a "race track" filtering algorithm. The algorithm removes cycles with a local range between successive extrema that is less than a selected "threshold" value. In the technique used here, the operator sets the threshold to define those cycles that may be eliminated from the record. Figure 4 illustrates the extrema retained from the data set shown in Figure 3 when the threshold is set to 6.2 MPa. As a "rule-of-thumb," the threshold is set to the root-mean-square (RMS) of the oscillating stress (see discussion below). This procedure eliminates stress cycles that are insignificant in the fatigue calculation and significantly decreases the processing time for a data set. For the damage calculations presented here, no cycles

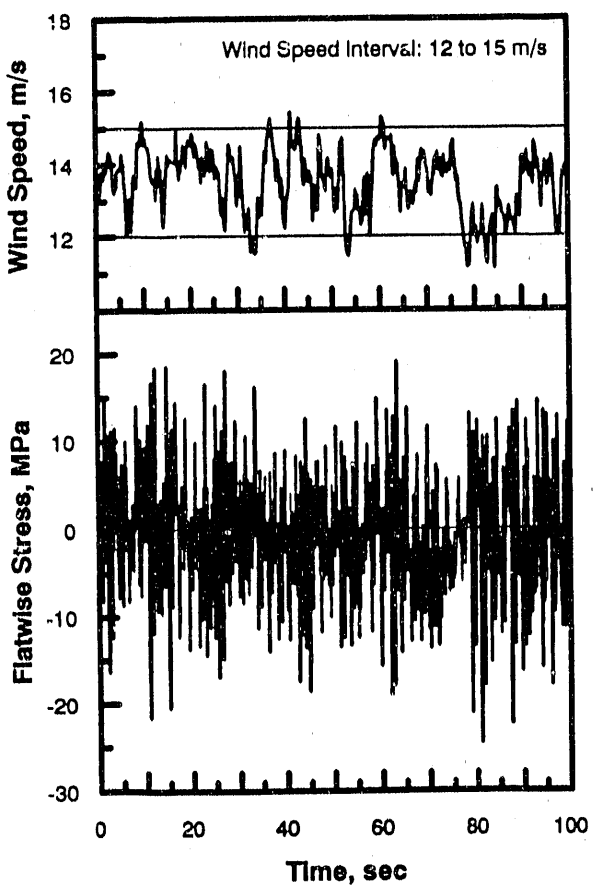

FIGURE 1: TYPICAL DATA RECORD

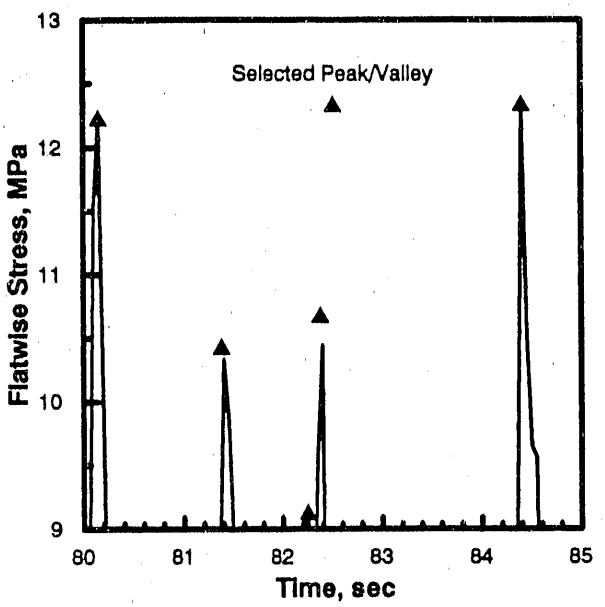

FIGURE 2: ESTIMATION OF TRUNCATED EXTREMA

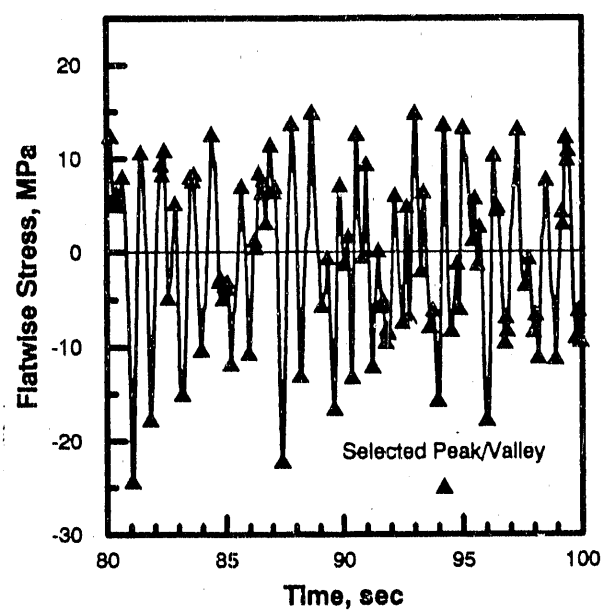

FIGURE 3: SELECTED EXTREMA WITH NO FILTER

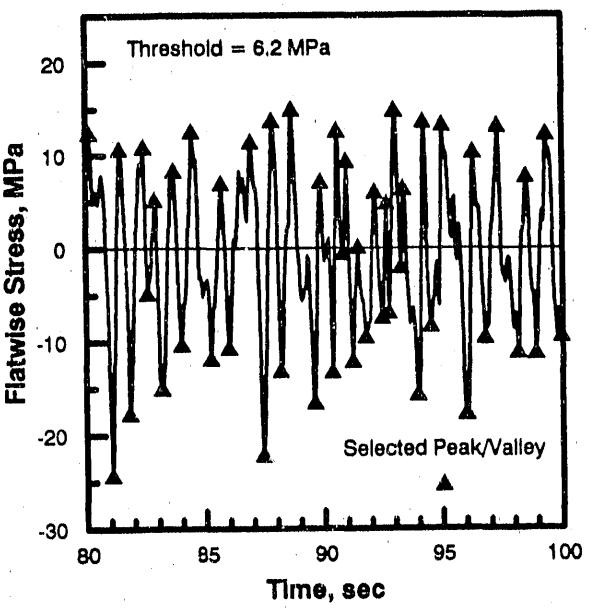

FIGURE 4: SELECTED EXTREMA WITH THRESHOLD OF 6.2 MPa

were eliminated from consideration; i.e., the threshold was set equal to zero.

Thus, the pre-count algorithms reduce the data record to a sequential list of peaks and valleys.

Counting Algorithm

The rainflow counting algorithm counts the number of closed stress/strain hysteresis loops in the data. The algorithm characterizes each stress cycle in the histogram by its mean value and its peak-to-peak range. To speed operation, the algorithm uses "one-pass" through the data to count the stress cycles; i.e., the peak-valley data are read only once during processing by the count algorithm.

Post-Count Algorithm

In the LIFE2 formulation, the cyclic stresses imposed on the turbine component are characterized by the magnitude of their mean stress and by the peak-to-peak range of their alternating stress components and by the operating condition of the turbine. The final algorithm maps each stress cycle into a series of cycle count matrices that are functions of these three variables.

EXAMPLE PROBLEM

Data records from the Sandia 34-m Test Bed are used here to illustrate the use of the rainflow counter for the analysis of the service lifetime of a turbine blade.

The Sandia 34-m VAWT

Sandia National Laboratories has erected a research oriented, 34-meter diameter, Darrieus VAWT near Bushland, Texas [8]. This variable speed turbine, commonly described as the 34-m Test Bed, has been operated at fixed speeds throughout its operating range of 28 to 38 rpm and in a true variable speed mode. The turbine and its site have been equipped with a large array of sensors that permit the characterization of the turbine under field conditions.

The highest stressed region of the blade, both in the flatwise and lead-lag directions, was found to be at the upper blade-to-tower joint (upper root) [9,10]. The upper root is where the 48 inch chord blade section attaches to the tower [8]. A detailed parametric study of the fatigue life of this joint was conducted in Reference 7. The predicted lifetimes for this joint, when the machine is operated in a constant speed mode of 28 rpm, 34 rpm and 38 rpm and a variable speed mode (labeled Var), are shown in Table I. This table is adapted from Reference 7. This set of predictions is based on "measured" data with the turbine located at the test site in Bushland. A complete set of the assumptions used to obtain these predictions are presented in Reference 7.

TABLE I: SERVICE LIFETIME FOR VARIOUS OPERATION ALGORITHMS

Service Lifetime (yrs)	Operation Algorithm			
	28 rpm	34 rpm	38 rpm	Var
Flatwise	966.	504.	286.	391.
Lead-Lag	296000.	9470000.	73.9	494.

For the example presented in this manuscript, the flatwise stress state for the joint will be analyzed with constant speed operation at 28 rpm; i.e., the critical stress state in fatigue for this mode of turbine operation.

Strain Gauge Data

The stress states for the upper root were measured using strain gauges located 0.91 m from the blade root [8]. This gauge set measured the flatwise bending stress. To convert these bending stress data to total stress data requires three correction factors: one each to correct for gravity, tensile stresses and stress concentrations. All data presented here contain these correction terms.

Gravity: The strain gauge data used here are referenced to a stopped turbine with no wind and with the blades attached to the turbine. Thus, these data do not contain the stress component imposed upon the blade by gravity (see the discussion in Reference 11). For the upper joint, the gravity stress component at the gauge section was measured to be 43.8 MPa and calculated to be 42.1 MPa [11]. For the analysis presented here, the measured gravity stress component was added directly to the raw data before counting.

Tensile Stress: The tensile stress component at the gauge section, due to the rotation of the turbine at a constant speed of 28 rpm, has been calculated to be 4.98 MPa at the upper joint [10]. This stress component was also added directly to the raw data before counting.

Stress Concentration: The strain gauge set used for the data analyzed here is located 0.91 m from the blade root [8]. The measured, flatwise bending stress data were increased by an analytically-derived factor of 1.23 to adjust them to the true root location [7,10]. This correction term was applied to the data after the other two correction terms were added to them.

Operational Stress States

Wind Speed Intervals: As anticipated and illustrated in Figure 1, the wind speed at the Bushland site is not constant for even relative short time periods. Thus, to construct a set of stress cycle count matrices (as a function of wind speed) for this turbine requires that relatively short time-series-data segments be extracted from data records.

Based on available data records and the variations of wind speeds at the Bushland site, six wind speed intervals were chosen to cover the operating range of this turbine. These intervals are summarized in Table II.

Table II. Summary of Wind Speed Intervals

Wind Speed Interval (m/sec)	Data Seg	Total Time (sec)	Stress Summary (MPa)			
			Rainflow		Bins	
			Mean	RMS	Mean	RMS
5-7	2	600	0.5	2.2	-1.1	2.2
7-9	2	750	-1.2	2.8	-1.1	3.1
9-12	3	445	-1.5	4.8	-1.1	4.5
12-15	5	700	-1.0	6.2	-1.1	6.6
15-18	5	680	-2.5	9.4	-1.1	8.9

As discussed in Reference 7, the normal operating range of the turbine extends to a wind speed of 20 m/s. As the time-series data records in the 18 to 20 m/s wind speed interval were very short (due to the extreme variability of the wind at this speed), a rainflow analysis was not attempted for this wind speed interval.

Data Segments: As seen in Figure 1, even this relatively coarse grid does not preclude some excursions outside of the wind speed interval of interest. Thus, to obtain time series of sufficient length for analysis (a minimum of 200 turbine rotations), several data segments were extracted from one or more relatively long (at least 1200 sec) stress-time data records. Each segment was chosen to have an average value near the center of its respective wind speed interval and to have minimal excursions outside that interval. The number of segments used in each interval are summarized in Table II (labeled "Data Seg" in the table).

In general, the wind speed held closer to an average value in the low wind speed intervals, thus fewer data segments were required for the low wind speed intervals than for the high wind speed intervals. The time length of the individual data segments ranged from 500 sec (for a segment in the 5 to 7 m/s wind speed interval) to 60 sec (in the 15 to 18 m/s interval).

Time Intervals: As stated above, the total duration of the data segments in each wind speed interval was a minimum of 420 seconds; i.e., at least 200 turbine rotations. To further insure that the total duration of the time series data was sufficiently long for this analysis, the distribution of the alternating stress cycle range was monitored as a function of the total time contained in the data segments. A typical plot of these data, for the 12 to 15 m/sec wind speed interval, is shown in Figure 5. In this figure, the cycle counts are summed in 2 MPa intervals. To allow direct comparison of the data counted over various time lengths, the cycle counts are normalized to a 100 second time interval. As seen in this plot, the distribution of stress cycles converges to a steady state distribution as the total length of the time series data increases. The total duration of the data used in each wind speed interval is summarized in Table II (labeled "Total Time" in the table).

In Figure 5, the data segments were counted first and then added together. Another test case was run in which the data segments were placed "back-to-back" and were then counted as a single data set. The result was identical to that shown as the solid line in Figure 5.

Mean Stress: The mean stresses measured for the rainflow counted stress histories are listed in Table II. The table compares the mean of these relatively shot duration data with "bins" data that are based upon several hundred hours of

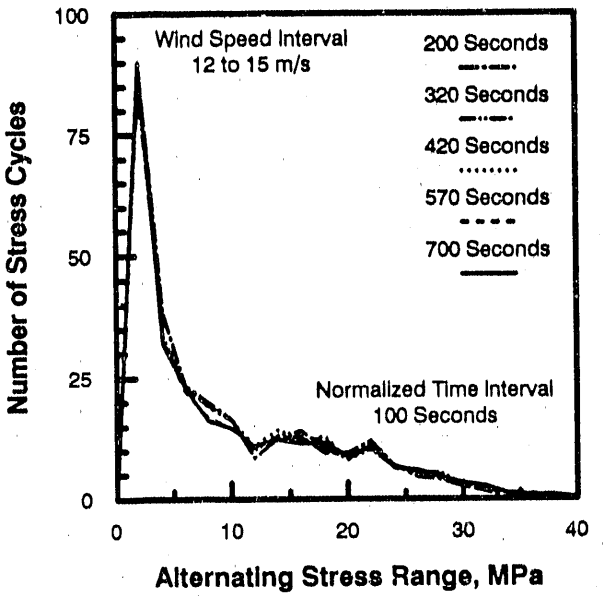

FIGURE 5: STRESS CYCLES COUNTED IN A SERIES OF INTERVALS

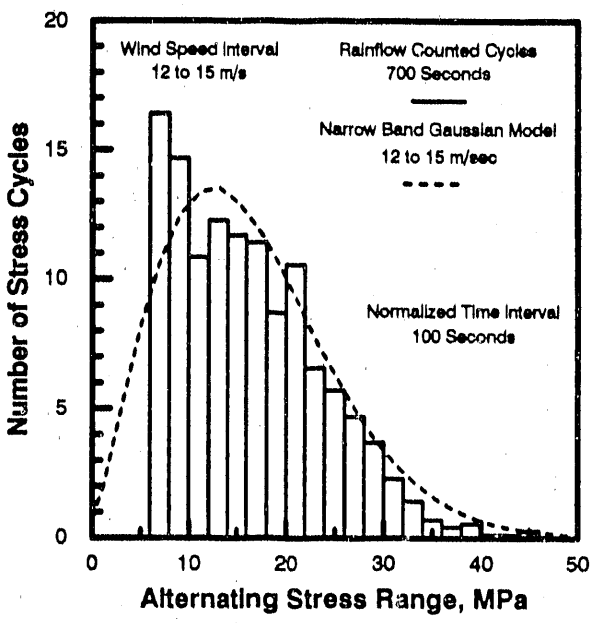

FIGURE 6: COUNTED AND PREDICTED STRESS CYCLES

turbine operation [9,10]. As shown in the table, the mean of the rainflow counted data is in very good agreement with the bins data.

RMS Stress: A measure of the distribution of the stress cycles imposed upon the turbine component is the root-mean-square (RMS) of the oscillating stress after the mean stress is removed [9]. The RMS values computed for the rainflow counted data are summarized in Table II.

The RMS may also be compared to bins data presented in References 9 and 10. However, the data presented in these references are based on relatively small wind speed intervals of 0.5 m/s. To permit the direct comparison of data, several bins data sets were "added" together to obtain a composite RMS value for the wind intervals used here. These values are also reported in Table II.

As seen in Table II, the agreement between the bins data and the rainflow counted data is very good.

Narrow-Band Gaussian Model: The operating stresses on the turbine have been modeled using a narrow-band Gaussian approximation [3,12]. This model yields a Rayleigh distribution for the peak-to-peak range of the cyclic stresses. The distribution of the ranges in the rainflow counted data for the 12 to 15 m/s wind speed interval are compared to model predictions in Figure 6. The cycles in both distributions are counted in 2 MPa intervals. The low stress counts in the rainflow counted distribution have been eliminated from Figure 6 because they do not contribute significantly to fatigue damage and they are not modeled by this approximation.

As discussed above, the rainflow counts do not compare directly to a single Rayleigh distribution. To permit a direct comparison of data, several Rayleigh distributions were added together to obtain a composite distribution for the wind speed intervals used here. The composite distribution for the 12 to 15 m/s wind speed interval is the distribution shown in Figure 6.

Similar to Figure 5, the cycle count has been normalized to a 100 second time interval to allow direct comparison of the data counted over various time lengths.

As seen in Figure 6, the distributions compare favorably.

Prediction of Service Lifetime: The service life predictions listed in Table I are based on a cut-out wind speed of 20 m/s. But, the time-series data records do not include data for the 18 to 20 m/s wind speed interval. Rather than exclude this interval from the analysis, the narrow-band Gaussian model was used to fill out the wind speed intervals for the rainflow cycle count matrices. Keeping all other parameters constant, the predicted service lifetime based on the rainflow analysis was 2180 years, see Table III.

The prediction of service lifetime based on the rainflow counted cycles is over a factor of two greater than that predicted by the Gaussian

TABLE III: SERVICE LIFETIME PREDICTIONS FOR THE UPPER ROOT

Service Lifetime (yrs)	Operational Stresses	Start-Stop Cycles	
		Braking Stops	Prop Braking Stops
Gaussian	966	721	903
Rainflow	2180	1230	1890

model. As shown in Table II and in Figure 6, the differences between the two distributions are relatively slight. However, for the prediction of service lifetimes, the significant difference between the two lies in the large alternating stress region, see Figure 6. In the high stress region, the Gaussian distribution yields a long "tail." In this region, the model predicts that the turbine will be subjected to some very high stress cycles over the course of its lifetime. Although the frequency of occurrence for these high stress cycles is very small, it is finite, and they significantly affect the predicted service lifetime for a WECS component. The rainflow counted data has the same nominal distribution but the high stress tail of the Gaussian distribution is sparsely populated.

This observation is not to say that the entire high stress region of the rainflow counted data is devoid of cycle counts. Some relatively large stress cycles were counted in each wind speed interval. For the data reported here, the ratios of the peak-to-peak range of the largest stress cycle to the RMS value are 7.6, 7.9, 7.9, 9.3 and 8.0 for the wind speed interval 5 to 7, 7 to 9, 9 to 12, 12 to 15 and 15 to 18 m/s, respectively.

The increase in the predicted service lifetime of a WECS component that is due to the sparse population of rainflow counted data in the high stress region has been noted previously by Malcolm [13]. Moreover, Malcolm has suggested that the high stress tail of the Gaussian distribution not be included in this model for the operating stresses on the turbine. He suggests terminating the distributions at approximately 6 times the RMS value for the lead-lag stress and 8 times the RMS value for the flatwise stress. Based on the data presented here, this observation is correct; however, these data, and the data presented by Malcolm, are based on stress-time histories that are extremely short when compared to the anticipated frequency of occurrence for the high stress cycles. A Rayleigh probability distribution predicts that a stress cycle with a range of 6 times the RMS value occurs once in 3,000 cycles (approximately once each hour of turbine operation at 28 rpm). With a range of 9 times the RMS value, the cycle is predicted to occur once in 25,000 stress cycles (approximately once in 8 hours of operation). Thus, the sparse population in the high stress tail may be due to the short duration of the time series data. Elimination of the high stress tail in the Gaussian distribution appears to be premature at this time.

Transient Stress States

The incorporation of the rainflow counting algorithm into the LIFE2 code permits the inclusion of entirely new classes of stress states into the analysis scheme of this code. The important class of transient stress states used in this illustrative example is the start-stop cycle for the turbine. A typical stopping cycle for the Test Bed is shown in Figure 7.

As reported by Vachon [14], the number of start-stop cycles for the turbine varies over a very large range, depending upon the particulars of the control algorithm used to regulate the turbine. Typically, the number of start-stop cycles is estimated to be in the range of a few thousand cycles per year. For this example, we will assume that the turbine has 2500 start-stop cycles each year.

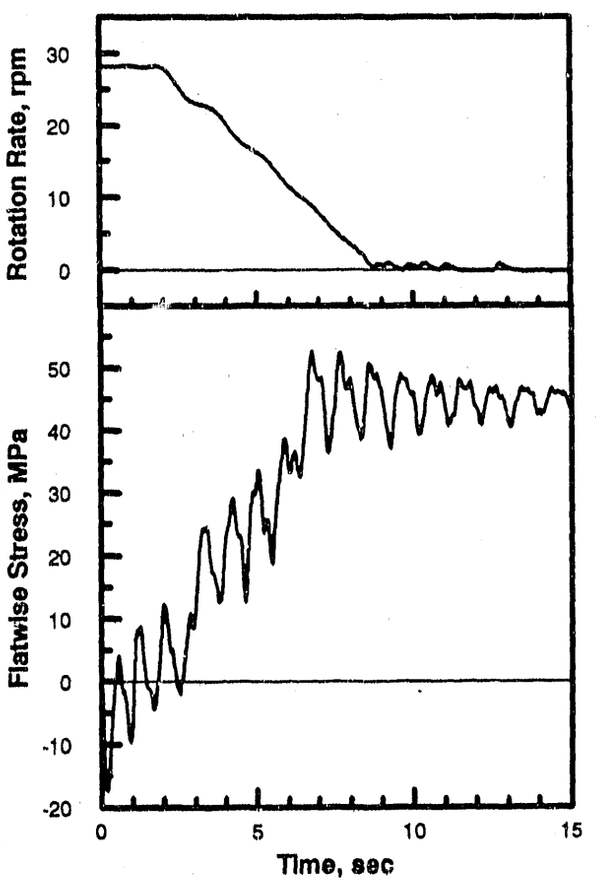

FIGURE 7: TYPICAL RECORD FOR A BRAKING STOP

The Sandia 34-m Test Bed is a variable speed machine with programable controls [8]. Under normal operating conditions, the acceleration and deceleration of the turbine is accomplished relatively slowly, requiring many minutes to start or stop the turbine. Under "alarm" conditions, the turbine is stopped by its brakes in a few seconds (Figure 7 is one of these stops). Each one of these events, herein called standard start, proportional braking stop and braking stop, respectively, was analyzed using the rainflow counting algorithm.

For all three of these events, and as illustrated in Figure 8, the distribution of stress cycles in their respective cycle count matrices was highly non-uniform. In all cases, all but one stress cycle had a relatively small amplitude. That single high stress cycle had a amplitude of 42.9, 46.3 and 70.2 MPa for the standard start, proportional braking stop and braking stop, respectively.

Prediction of Service Lifetime: The predicted service lifetime for the upper joint, based on several operating and start-stop scenarios, are summarized in Table III. The start-stop cycles were added to both the rainflow and the Gaussian operating stress states. Two stopping scenarios were examined here. In the first case, only braking stops were available and in the second case, the two classes of stops were available. In both scenarios, only the standard start cycle was used.

In the first case, it was assumed that only the braking system was available to stop the turbine.

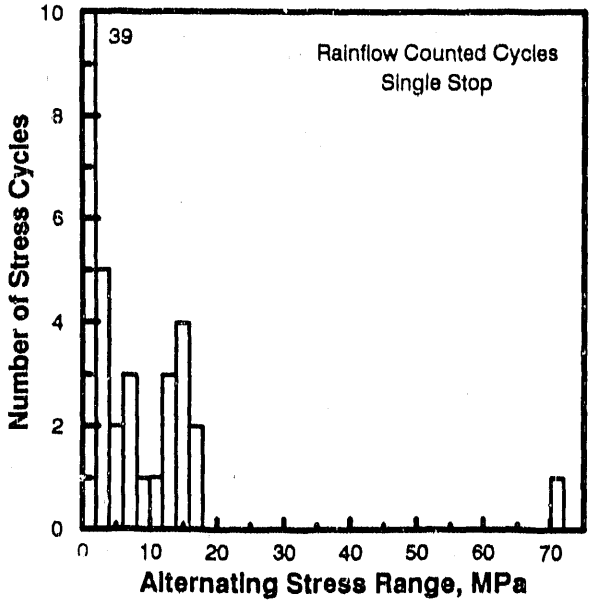

FIGURE 8: COUNTED STRESS CYCLES FOR BRAKING STOP

This case more closely approximates a single speed turbine. The results of the service life predictions are listed in Table III under the heading "Braking Stops."

In the second case, both classes of stops are available. This case more closely approximates a variable speed turbine. Here, we assume that 80 percent of the stops were proportional braking stops and the remainder were braking stops. The results of the fatigue life analyses are listed in Table III under the heading "Prop Braking Stops."

As seen in Table III, the inclusion of start-stop cycles does influence the predicted service lifetime of the joint. The ability of the turbine's control system to handle transient events with proportional controls increases the service lifetime of the turbine.

SUMMARY

A set of algorithms that permit the analysis of time-series stress data has been incorporated into the LIFE2 fatigue/fracture analysis code. The algorithms are built around a rainflow counting algorithm. Data from the Sandia 34-m Test Bed are used to illustrate the features of the algorithms. The results of the rainflow analysis are compared and contrasted to previously reported predictions for the service lifetime of the fatigue critical component for this turbine.

REFERENCES

1. Downing, S. D., and Socie, D. F., "Simple Rainflow Counting Algorithms", *International Journal of Fatigue*, Vol. 4, N. 1, 1982, pp. 31-40.

2. Schluter, L. L., and Sutherland, H. J., "Reference Manual for the LIFE2 Computer Code," SAND89-1396, Sandia National Laboratories, Albuquerque, NM, September 1989, 170 p.

3. Sutherland, H. J., "Analytical Framework for the LIFE2 Computer Code," SAND89-1397, Sandia National Laboratories, Albuquerque, NM, September 1989, 42 p.

4. Schluter, L. L., and Sutherland, H. J., "Rainflow Counting Algorithm for the LIFE2 Fatigue Analysis Code," *Proceedings of the Ninth ASME Wind Energy Symposium*, D. E. Berg (ed), SED-Vol. 9, ASME, January 1990, pp. 121-123.

5. Schluter, L. L., and Sutherland, H. J., *Rainflow Counting for the LIFE2 Fatigue Analysis Code*, SAND90-2259, Sandia National Laboratories, Albuquerque, NM, in publication.

6. Schluter, L. L., *Programmer's Guide for LIFE2's Rainflow Counting Algorithm*, SAND90-2260, Sandia National Laboratories, Albuquerque, NM, in publication.

7. Ashwill, T. D., Sutherland, H. J., and Veers, P. S., "Fatigue Analysis of the Sandia 34-Meter Vertical Axis Wind Turbine," *Proceedings of the Ninth ASME Wind Energy Symposium*, D. E. Berg (ed), SED-Vol. 9, ASME, January 1990, pp. 145-151.

8. Ashwill, T. D., et al, "The Sandia 34-Meter VAWT Test Bed", *Proceedings of Wind Power '87*, American Wind Energy Association, SERI/CP-217-3315, January 1987, pp. 298-308.

9. Ashwill, T.D., "Initial Structural Response Measurements for the Sandia 34-Meter VAWT Test Bed," *Proceedings of the Eighth ASME Wind Energy Symposium*, D. E. Berg and P. C. Klimas (eds), SED-Vol. 7, January 1987, ASME, pp. 285-292.

10. Ashwill, T.D. and Veers, P.S., "Structural Response Measurements and Predictions for the Sandia 34-Meter Test Bed," *Proceedings of the Ninth ASME Wind Energy Symposium*, D. E. Berg (ed), SED-Vol. 9, ASME, January 1990, pp. 137-144.

11. Sutherland, H. J., and Ashwill, T. D., "A Comparison of the Predicted and Measured Gravitational Stresses in VAWT Blades," *Proceedings of the Seventh ASME Wind Energy Symposium*, A. H. P. Swift and R. W. Thresher (eds), ASME, January 1988, pp. 125-126.

12. Veers, P. S., "Simplified Fatigue Damage and Crack Growth Calculations for Wind Turbines," *Proceedings of the Eighth ASME Wind Energy Symposium*, D. E. Berg and P. C. Klimas (eds), SED-Vol. 7, ASME, January 1987, pp. 133-140.

13. Malcolm, D. J., "Predictions of Peak Fatigue Stresses in a Darrieus Rotor Wind Turbine Under Turbulent Winds," *Proceedings of the Ninth ASME Wind Energy Symposium*, D. E. Berg (ed), SED-Vol. 9, ASME, January 1990, pp. 125-135.

14. Vachon, W. A., "The Effect of Controls on Life and Energy Production of the 34-m VAWT Test Bed, " *Proceedings of the Eighth ASME Wind Energy Symposium*, D. E. Berg and P. C. Klimas (eds), SED-Vol. 7, January 1987, ASME, pp. 209-218.

DISCLAIMER

-END-

DATE FILMED

11/05/90